Title

Nanoparticle-programmed self-destructive neural stem cells for glioblastoma targeting and therapy.

Journal

Small, 9(24)

Authors

Cheng, Yu
Morshed, Ramin
Cheng, Shih-Hsun
et al.

Publication Date

2013-12-20

DOI

10.1002/smll.201301111

Peer reviewed

Published in final edited form as:
Small. 2013 December 20; 9(24): . doi:10.1002/smll.201301111.

Nanoparticle-Programmed Self-Destructive Neural Stem Cells for Glioblastoma Targeting and Therapy

Dr. Yu Cheng,
The Brain Tumor Center, The University of Chicago, Chicago, Illinois, USA

Ramin Morshed,
The Brain Tumor Center, The University of Chicago, Chicago, Illinois, USA

Dr. Shih-Hsun Cheng,
Department of Radiology, The University of Chicago, Chicago, Illinois, USA

Alex Tobias,
The Brain Tumor Center, The University of Chicago, Chicago, Illinois, USA

Dr. Brenda Auffinger,
The Brain Tumor Center, The University of Chicago, Chicago, Illinois, USA

Dr. Derek A. Wainwright,
The Brain Tumor Center, The University of Chicago, Chicago, Illinois, USA

Lingjiao Zhang,
The Brain Tumor Center, The University of Chicago, Chicago, Illinois, USA

Catherine Yunis,
The Brain Tumor Center, The University of Chicago, Chicago, Illinois, USA

Yu Han,
The Brain Tumor Center, The University of Chicago, Chicago, Illinois, USA

Prof. Chin-Tu Chen,
Department of Radiology, The University of Chicago, Chicago, Illinois, USA

Prof. Leu-Wei Lo,
Division of Medical Engineering, National Health Research Institute, Taiwan

Prof. Karen S. Aboody,
Department of Neuroscience, City of Hope National Medical Center and Beckman Research Institute Duarte, California, USA

Dr. Atique U. Ahmed, and
The Brain Tumor Center, The University of Chicago, Chicago, Illinois, USA

Prof. Maciej S. Lesniak
The Brain Tumor Center, The University of Chicago, Chicago, Illinois, USA

Chin-Tu Chen: c-chen@uchicago.edu; Maciej S. Lesniak: mlesniak@surgery.bsd.uchicago.edu

Correspondence to: Chin-Tu Chen, c-chen@uchicago.edu; Maciej S. Lesniak, mlesniak@surgery.bsd.uchicago.edu.

YC, RM and S-HC contributed equally to this work.

Supporting Information
Supporting Information is available from the Wiley Online Library or from the author.

Patients with glioblastoma multiforme (GBM), the most common and aggressive form of adult brain cancer, suffer from poor outcomes, even after undergoing surgery or radiotherapy in conjunction with chemotherapy.[1] In the context of GBM treatment, nanoparticles offer the potential to improve drug delivery by increasing drug half-life and allowing for controlled release.[2] However, achieving extensive yet specific drug distribution in a tumor is still a major challenge for such systems, especially when targets including diffuse infiltrating cancer cells are distant from the site of administration. While diffusion-based delivery of these systems has been attempted, it often results in poor intratumoral distribution and an inability to reach distant metastatic sites.[3] Thus, in order to maximize the therapeutic potential of drug-nanoparticle conjugates while minimizing drug-related side effects, a targeted delivery strategy is needed to ensure that only malignant tissue in the brain is affected.

Neural stem cells (NSCs), with their inherent tumor-tropic migratory capability,[4] may offer an innovative approach for targeted delivery of anti-cancer drug-loaded nanoparticles to distant and diffuse tumor sites. Several groups, including our own, have reported the use of various targeted delivery approaches using NSCs as vehicles in xenograft models of human glioma.[5] However, the use of such cell carriers in the drug delivery field of nanoparticle-mediated chemotherapy is limited. While a few studies have demonstrated the use of mesenchymal stem cells to deliver drug-loaded nanoparticles through intratumoral administration,[6] no previous work has shown this concept using NSCs. For such a system to work, it is critical to choose a platform that delays drug-release so that the drug-related toxicity does not impair migratory function. Upon arrival at the tumor site, stem cell carriers must be able to release the drug to affect neighboring cancerous cells in the nearby vicinity. Mesoporous silica nanoparticles (MSNs) possessing controlled-release capabilities and non-toxic features can serve as a platform to meet these criteria.[7–10]

In the context of glioma therapy, pH-sensitive drug release is a suitable mechanism for non-invasively triggering programmed cell death when compared to the external triggers such as light, which is limited by poor penetration depth across the cranial vault. There is a significant difference in the environmental pH between cancerous and normal tissues: pH in tumor tissue is approximately 6.8–7.0, which is lower than normal physiological pH 7.4.[11] In addition, acidic compartments within cells, such as endosomes and lysosomes, have a pH between ~4.5–6 and are important organelles for drug-release intracellularly.[12]

Here, we report an in vivo model of loading the HB1. F3.CD NSC line (approved by FDA for human clinical trials via local injection, Identifier: NCT01172964) with pH-sensitive doxorubicin-loaded mesoporous silica nanoparticles (MSN-Dox). This combination promoted programmed self-destruction of HB1.F3.CD carriers that had migrated to glioma cells after local injection based on the FDA-guided human clinical trials (Scheme 1). To achieve this, we first designed an 80 nm MSN with highly ordered nano channels, allowing for a high drug-loading capacity. Doxorubicin (Dox) was selected due to its high anti-tumor potency when compared to the current standard-of-care drug, temozolomide (TMZ) (Figure S1 in the Supporting Information).[13] Dox was subsequently linked to the surface of MSNs via a pH-sensitive hydrazone bond.[7] The outermost surface of MSNs was further modified with trimethylammonium (TA) groups, which increased the surface charge (zeta potential +3.78 ± 5.2 mV at pH 7.4, Supporting Information Table S1) and allowed for improved cellular uptake. According to transmission electron microscopy (TEM) imaging, MSN-Dox conjugates were well dispersed with an average diameter of 80 nm and with highly ordered nanochannels on their surface (Figure 1a). The drug loading percentage of MSN-DOX was 1.05 wt%. The surface area was 510 m^2/g and pore size was 3.5 nm as determined by Brunauer–Emmett–Teller and Barrett–Joyner–Halenda methods, respectively (Table S1). Drug-release kinetics of MSN-Dox was both pH- and time-dependent (Figure 1b). Under

acidic pH, the hydrazone bond between the drug and MSNs was hydrolyzed, generating Dox in its active form. Within the first 6 h, MSN-Dox conjugates were stable with less than 10% release at physiological pH 7.4, but when exposed to pH 1, over 95% of bound drug was released within the same time period. Between pH 4.5 and 5.5 (corresponding to the pH within cellular lysosomes),[12] drug release was sustained and increased over the first 48 h, and by 120 h, 50–70% of drug molecules had been released from MSNs (Figure 1b). Thus, the pH-responsive MSN-Dox conjugates provided prolonged release of Dox within a pH range corresponding to that found in the lysosomes of cells.

It was critical to ensure that the MSN-Dox conjugates were adequately endocytosed by HB1.F3.CD cells and trafficked to the lysosomes where the low pH organelles would facilitate efficient drug release. Flow cytometry was used to assess the proportion of HB1.F3.CD cells that endocytosed the conjugate. After 4 h of incubation, 88.1% of HB1.F3.CD cells demonstrated significant uptake of the nanoparticle constructs (Figure 1c). This was comparable to the free Dox incubation condition in which 98.4% of cells displayed uptake of the drug (Figure S2). Confocal microscopy was used to assess intracellular trafficking (Figure 1d). Immediately after a 4 h incubation, some of the MSN-Dox conjugates appeared to be adsorbed onto the cell membrane while others already appeared to be localized to the lysosomes with a Pearson's correlation coefficient of 0.56 ± 0.08. At 24 h post-incubation, the Pearson's correlation coefficient of Dox and Lysotracker Green location was 0.81 ± 0.03 ($p < 0.01$ compared to 0 hr) (Figure 1e), suggesting the release of Dox and MSN-Dox still localized to the lysosomes. Based on the pH-sensitive releasing mechanism, one might expect approximately 50% Dox release from MSNs at 24 h after incubation in a lysosomal pH of 4.5 (Figure 1b). It is also probable that a small amount of the drug is released within endosomes during transport to the lysosomes, since the late endosome has a pH of approximately 5.5.[14]

In order to allow for migration of the NSC carrier towards invading tumor cells, MSN-Dox toxicity needed to be delayed by about 24–48 h. To assess this, HB1.F3.CD cells were incubated in MSN-Dox or free Dox at a concentration equal to the average loading concentration on MSNs. Compared to free Dox, MSN-Dox conjugates delayed the drug-related toxicity to the cellular carrier over the first 72 h (Figure 2 and Figure S3). By 96 h, the percentage of viable HB1.F3.CD cells in the MSN-Dox conditions was comparable to that seen in the free Dox incubation conditions (Figure S3), demonstrating a similar end-point of overall toxicity. The release profile of Dox from the MSN-Dox loaded HB1.F3.CD cells (Figure S3B) was consistent with cell death (Figure S3C) over a 72-h period. At 0 h, there was no significant amount of Dox released from the cells. 0.27 ± 0.016 μM Dox was released from MSN-Dox loaded NSC after 24 h and the concentration slightly increased to 0.33 ± 0.017 μM after 48 h. The released Dox concentration reached 0.64 ± 0.03 μM after 72 h. When the cells were dying, the released Dox concentration increased. Furthermore, the released Dox in the media should be sufficient to cause death of U87 glioma cells (IC50 = 0.3 μM). MSN-Dox-loaded HB1. F3.CD cells also showed tumor-specific homing capabilities within 20 h in vitro. Microscopic images and quantification of migratory distance over 20 h are depicted in Figure 2 and S4. MSN-Dox-loaded HB1.F3.CD cells migrated toward U87 glioma cells at a rate similar to unloaded HB1.F3.CD cells. It is important to note that MSN-loaded HB1.F3.CD cells also migrated to the glioma cells while free Dox induced significant cell-death within this time period (Figures S4 and 2c), demonstrating the importance of drug conjugation to MSNs. These in vitro results demonstrate that conjugation of Dox to MSNs delays drug toxicity toward the NSC carrier long enough to allow for migration to occur and can provide a self-destruct mechanism after migration is completed.

The cytotoxicity of MSN-Dox-loaded HB1.F3.CD cells towards U87-GFP-Luc was evaluated using a co-culture experiment (schematic depicted in Figure S5). There was a visible decrease over time in the amount of U87-GFP-Luc cells when co-cultured with MSN-Dox-loaded HB1.F3.CD cells as indicated by fluorescence images (Figure 3a). By 96 h, a significant decrease in U87 cell viability was observed in the MSN-Dox-loaded HB1.F3.CD cell incubation conditions, as quantified by the analysis of luciferase activity (Figure 3b). Dox transfer from HB1.F3.CD cells to U87 cells was also studied using confocal microscopy (Figure 3c). By 24 h, MSN-Dox-loaded HB1.F3.CD cells had targeted U87 cells and had shown some morphological changes that most likely represented cytotoxicity towards the carrier due to drug-release from MSNs. Dox fluorescence was also observed in adjacent U87 cells at this time point, demonstrating that some of the MSN-Dox conjugates were being transferred from the NSC carriers to the glioma cells. After 48 h, less HB1.F3.CD cells were visualized and Dox fluorescence was observed in the surrounding U87 cells. These results were even more apparent by 72 h. Interestingly, Dox appeared to be localized in the nuclei and perinuclear region of U87 cells (Figure 3c), indicating that Dox on the MSNs had been released from lysosomes and had translocated to the nucleus. Although our study can explicitly demonstrate the delivery mechanism, such a complicated trilogy including MSN-Dox endocytosis to NSCs, migration and programmed NSC death, MSN-Dox release, and endocytosis by glioma cells comprises too many variables making the quantification of final drug concentration in tumor cells difficult. However, with the current experimental design, we can still observe the cytotoxicity of MSN-Dox on the glioma cells via NSC delivery. The delayed drug-transfer observed via confocal microscopy was consistent with results from our cytotoxicity assays using the same co-culture system.

Next, we wanted to demonstrate that MSN-Dox could be delivered to tumor cells using NSCs in an orthotropic human glioma xenograft model (Figure 4). Firefly luciferase-labelled HB1.F3.CD cells loaded with MSN-Dox were injected into the cerebral hemisphere contralateral to that of the tumor (a distance of 5 mm). The NSC migratory pattern was monitored via bioluminescence imaging (Figure 4a). Contralaterally-injected MSN-Dox-loaded HB1.F3.CD cells were found at the brain tumor site within 4 h after injection and this localization was even more robust by 24 h post-injection. Histological studies further revealed that Dox had been delivered into the tumor area as well (Figure 4b and Figure S6). Dox fluorescence was distributed around the border and within the tumor by 72 h after injection and persisted in the tumor for at least 10 days (Figure S7). Furthermore, there was no detectable amount of Dox in normal brain tissue expect for that immediately surrounding the tumor (Figure 4b and S6). This peri-tumoral Dox distribution may represent NSC delivery of the conjugates to invading glioma cells that are infiltrating the normal tissue surrounding the tumor. These results confirmed the delivery of the MSN-Dox via tumor-tropic HB1.F3.CD carrier cells over a distance of 5 mm. In addition, Dox distribution within the tumor after intratumoral injection of MSN-Dox-loaded HB1.F3.CD cells was studied (Figure S8). Dox fluorescence was found in the tumor area 3 days and 10 days after injection. This indicated that specific and extensive distribution of MSN-Dox within the tumor could be achieved through the use of NSC carriers.

Furthermore, we observed that MSN-Dox-loaded HB1.F3.CD cells showed an anti-tumor effect by inducing apoptosis, as assessed by immunofluorescence staining using a cleaved caspase-3 antibody (Figure 4c and Figure S9). Apoptosis was detected mainly within the tumor in both contralateral and intratumoral post 3-day injected samples. The apoptotic area also corresponded to Dox distribution within the tumor (Figure 4c). The majority of Dox was found in the tumor area (96%) as quantified by ImageJ. In addition, 96.5% of the apoptotic cells were found at the tumor site. Less than 4% of apoptotic cells were in the normal brain as shown in Figure 4c and Figure S9A. These data indicated that the pH-triggered mechanism was sufficient to delay the release of Dox for a period of time that

could enable migration of NSCs towards the tumor. MSN-Dox-loaded HB1.F3.CD cells preserved their tumor-tropic migratory properties and were able to release Dox upon arrival to the tumor, inducing apoptosis in the surrounding area. Analysis of adjacent sections indicated that the MSN-Dox-loaded HB1.F3.CD cells were extensively distributed throughout the tumor.

We chose to administer MSN-Dox-loaded HB1.F3.CD intracranially as opposed to systemically injection to demonstrate in vivo efficacy in order to circumvent problems associated with systemic distribution and drug side effects. The in vivo survival study demonstrated the advantage of using MSN-Dox-loaded HB1.F3.CD over MSN-Dox alone for glioma therapy as shown in Figure 5. We used PBS and MSN-Dox as controls and compared the overall survival outcomes of MSN-Dox-loaded HB1.F3.CD via two different methods of injection (intratumoral and contralateral injections). There were no significant changes in overall survival between the groups treated with MSN-Dox alone, when compared to the PBS group. Importantly, the MSN-Dox loaded HB1.F3.CD showed significant improvements over MSN-Dox groups for both intratumoral injection ($p = 0.03$) and contralateral injection ($p = 0.005$). The median survival of MSN-Dox loaded HB1.F3.CD group was prolonged to 41- and 42-days for intratumoral and contralateral injections, respectively. These results were consistent with the anti-tumor effect of MSN-Dox loaded HB1.F3.CD observed in the histology studies. Although this system has not been optimized for maximal efficacy in vivo, these preliminary results are encouraging and suggest the potential for stem cell carrier-based targeted delivery. Furthermore, while there may be some concern about the fate of these stem cells after administration, the system's self-destructing mechanism of action should prevent any future tumor-modulating effects by the NSCs. Introducing external triggers such as X-ray for drug release could be of value for future applications of this system. An additional imaging component to our set-up could also be implemented. Recently, versatile nanoparticle systems including gold nanoparticles and quantum dots were loaded into stem cells for photoacoustic imaging[15] and optical imaging.[16] Such a feature could also be incorporated into our system as well.

In summary, we have demonstrated the first example of targeted anti-cancer drug-nanoparticle conjugate delivery using NSC-based carriers in an orthotopic human glioma xenograft model. We first demonstrated that HB1.F3.CD cells could uptake MSN-Dox efficiently and that pH-controlled Dox release from the nanoparticle surface delayed drug-induced toxicity towards carrier cells, preserving their migratory function in vitro. Secondly, we established that MSN-Dox-loaded HB1.F3.CD cells could release MSN-Dox conjugates and cause significant toxicity to surrounding U87 glioma cells in vitro. Lastly, tumor-tropic migration of MSN-Dox-loaded HB1.F3.CD cells in an intracranial U87 xenograft mouse model was observed, resulting in the induction of apoptosis within tumors and improvements in survival. It should be noted that the HB1.F3.CD NSCs are restricted for clinic trials utilizing local injection for treatment of recurrent high-grade glioma based on the guidance of FDA. Such local injection of the nanoparticle-programmed NSCs enables these cells to disperse throughout the tumor via the tropic migration capacity of NSCs. Both intratumoral and contralateral injections are sufficient to achieve significant amounts of MSN-Dox-loaded NSCs in a tumor and elicit a significantly enhanced therapeutic effect compared to the MSN-Dox alone. We are currently conducting FDA guided pre-clinical studies based on this intracranial injection method in order to translate the MSN-Dox-loaded HB1.F3.CD cells for malignant glioma therapy. Taken together, this proof-of-concept study demonstrates that NSCs have the potential to serve as a novel delivery platform for multi-functional nanoparticles, allowing for targeting towards diffuse tumor sites after intracranial administration.

Acknowledgments

This work is supported by the National Institute of Neurological Disorders and Stroke U01NS069997 (MSL), R01NS077388 (MSL), K99 CA160775 (AUA) and F32 NS073366 (DAW). It is also supported by the National Health Research Institutes of Taiwan (MED-101-PP-04) and the National Science Council of Taiwan (NSC-100–2911-I-400–502). We thank the Integrated Microscopy Core Facility at the University of Chicago for technical support.

References

1. a) Grossman SA, Ye XB, Piantadosi S, Desideri S, Nabors LB, Rosenfeld M, Fisher J, Consortium NC. Clin Cancer Res. 2010; 16:2443–2449. [PubMed: 20371685] b) Wen PY, Kesari S. N Engl J Med. 2008; 359:492–507. [PubMed: 18669428]
2. a) Davis ME, Chen Z, Shin DM. Nat Rev Drug Discov. 2008; 7:771–782. [PubMed: 18758474] b) Zhang L, Gu FX, Chan JM, Wang AZ, Langer RS, Farokhzad OC. Clin Pharmacol Ther. 2008; 83:761–769. [PubMed: 17957183] c) Farokhzad OC, Langer R. ACS Nano. 2009; 3:16–20. [PubMed: 19206243]
3. Zhou JB, Atsina KB, Himes BT, Strohbehn GW, Saltzman WM. Cancer J. 2012; 18:89–99. [PubMed: 22290262]
4. a) Aboody KS, Brown A, Rainov NG, Bower KA, Liu SX, Yang W, Small JE, Herrlinger U, Ourednik V, Black PM, Breakefield XO, Snyder EY. Proc Natl Acad Sci USA. 2000; 97:12846–12851. [PubMed: 11070094] b) Lesniak MS. Expert Rev Neurother. 2006; 6:1–3. [PubMed: 16466305] c) Muller FJ, Snyder EY, Loring JF. Nat Rev Neurosci. 2006; 7:167–167.d) Ahmed AU, Lesniak MS. Expert Rev Neurother. 2011; 11:775–777. [PubMed: 21651324] e) Ahmed AU, Alexiades NG, Lesniak MS. Curr Opin Mol Ther. 2010; 12:546–552. [PubMed: 20886386]
5. a) Sonabend AM, Ulasov IV, Tyler MA, Rivera AA, Mathis JM, Lesniak MS. Stem Cells. 2008; 26:831–841. [PubMed: 18192232] b) Kranzler J, Tyler MA, Sonabend AM, Ulasov IV, Lesniak MS. Curr Gene Ther. 2009; 9:389–395. [PubMed: 19860653] c) Tyler MA, Ulasov IV, Sonabend AM, Nandi S, Han Y, Marler S, Roth J, Lesniak MS. Gene Ther. 2009; 16:262–278. [PubMed: 19078993] d) Ahmed AU, Rolle CE, Tyler MA, Han Y, Sengupta S, Wainwright DA, Balyasnikova IV, Ulasov IV, Lesniak MS. Mol Ther. 2010; 18:1846–1856. [PubMed: 20588259] e) Balyasnikova IV, Ferguson SD, Sengupta S, Han Y, Lesniak MS. PLoS One. 2010; 5:e9750. [PubMed: 20305783]
6. a) Li LL, Guan YQ, Liu HY, Hao NJ, Liu TL, Meng XW, Fu CH, Li YZ, Qu QL, Zhang YG, Ji SY, Chen L, Chen D, Tang FQ. ACS Nano. 2011; 5:7462–7470. [PubMed: 21854047] b) Roger M, Clavreul A, Venier-Julienne MC, Passirani C, Montero-Menei C, Menei P. Biomaterials. 2011; 32:2106–2116. [PubMed: 21183214] c) Gao Z, Zhang L, Hu J, Sun Y. Nanomedicine. 201210.1016/j.nano.2012.06.003d) Roger M, Clavreul A, Huynh NT, Passirani C, Schiller P, Vessieres A, Montero-Menei C, Menei P. Int J Pharm. 2012; 423:63–68. [PubMed: 21554935]
7. Lee CH, Cheng SH, Huang IP, Souris JS, Yang CS, Mou CY, Lo LW. Angew Chem Int Ed. 2010; 49:8214–8219.
8. Ashley CE, Carnes EC, Phillips GK, Padilla D, Durfee PN, Brown PA, Hanna TN, Liu JW, Phillips B, Carter MB, Carroll NJ, Jiang XM, Dunphy DR, Willman CL, Petsev DN, Evans DG, Parikh AN, Chackerian B, Wharton W, Peabody DS, Brinker CJ. Nat Mater. 2011; 10:389–397. [PubMed: 21499315]
9. Coti KK, Belowich ME, Liong M, Ambrogio MW, Lau YA, Khatib HA, Zink JI, Khashab NM, Stoddart JF. Nanoscale. 2009; 1:16–39. [PubMed: 20644858]
10. Slowing II, Vivero-Escoto JL, Wu CW, Lin VSY. Adv Drug Delivery Rev. 2008; 60:1278–1288.
11. Tannock IF, Rotin D. Cancer Res. 1989; 49:4373–4384. [PubMed: 2545340]
12. Fehrenbacher N, Jaattela M. Cancer Res. 2005; 65:2993–2995. [PubMed: 15833821]
13. Lesniak MS, Upadhyay U, Goodwin R, Tyler B, Brem H. Anti-cancer Res. 2005; 25:3825–3831.
14. Aubry L, Klein G, Martiel JL, Satre M. J Cell Sci. 1993; 105:861–866. [PubMed: 7691851]
15. Jokerst JV, Thangaraj M, Kempen PJ, Sinclair R, Gambhir SS. ACS Nano. 2012; 6:5920–5930. [PubMed: 22681633]

16. Yukawa H, Kagami Y, Watanabe M, Oishi K, Miyamoto Y, Okamoto Y, Tokeshi M, Kaji N, Noguchi H, Ono K, Sawada M, Baba Y, Hamajima N, Hayashi S. Biomaterials. 2010; 31:4094–4103. [PubMed: 20171733]

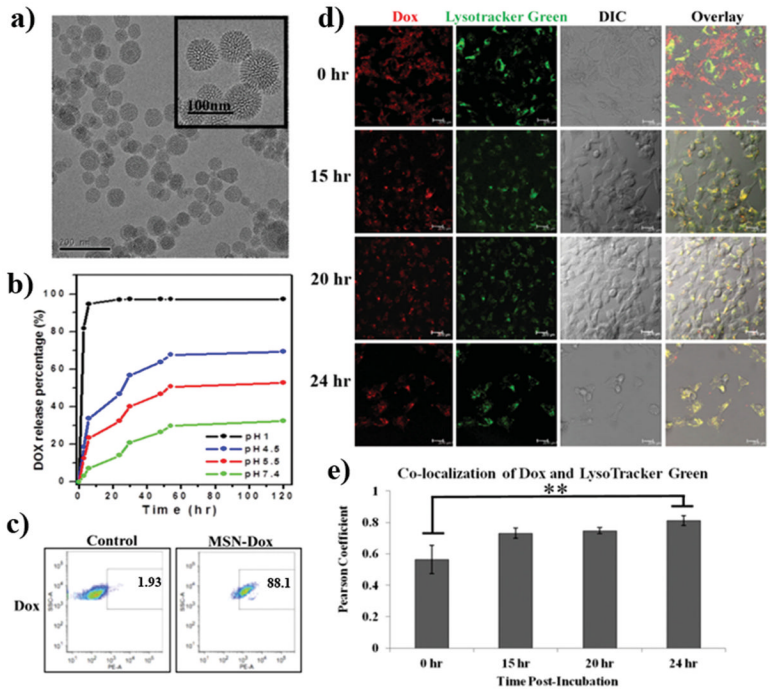

Figure 1.

MSN-Dox characterization and uptake into HB1.F3.CD neural stem cells. a) TEM image of MSN-Dox conjugates and b) the release profile of Dox from MSNs at varying pH. c) FACS data demonstrating significant HB1.F3.CD cell uptake of MSN-Dox after 4 h incubation. d) Confocal images of HB1.F3.CD cells after incubation with MSN-Dox. Scale bar: 20 μm. e) Pearson's correlation coefficient for Dox and LysoTracker Green location was determined using OpenLab. Co-localization increased over the first 24 h (**$p < 0.01$).

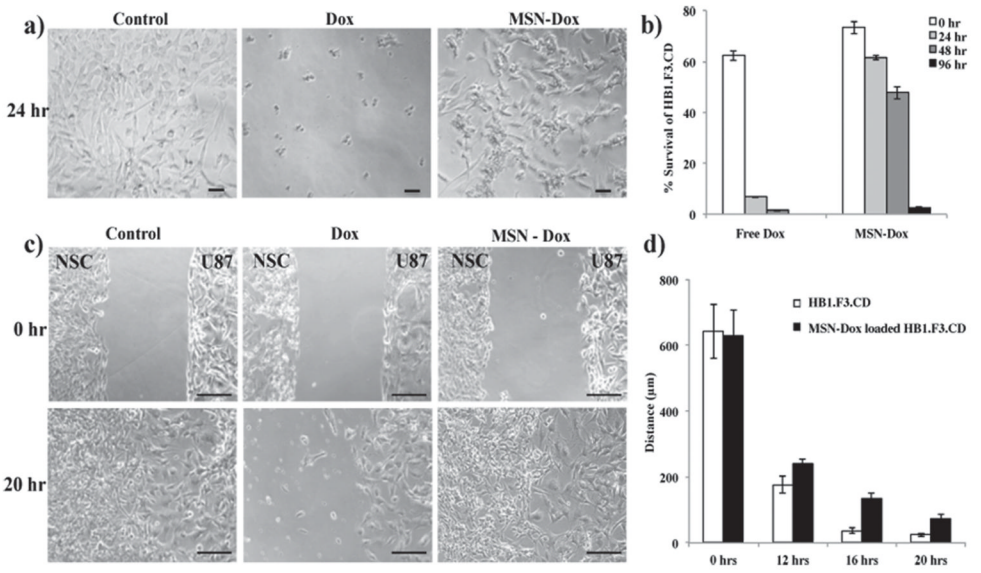

Figure 2.

Prolonged cell viability of MSN-Dox-loaded HB1.F3.CD (vs. free Dox) and the migratory ability to glioma cells. a) Light microscopy images demonstrating MSN-Dox and Dox toxicity towards HB1.F3.CD cells. b) MTT assay quantification of the time-dependent cell viability of MSN-Dox and Dox loaded HB1.F3.CD cells. c) Light microscopy images demonstrating Dox or MSN-Dox-loaded HB1.F3.CD cell migration towards U87 glioma cells. d) Quantitative results of migration of HB1.F3.CD and MSN-Dox loaded HB1.F3.CD. Distance measured was between the forefront of HB1.F3.CD and U87 cell lines. Scale bars: a): 20 μm; c): 200 μm.

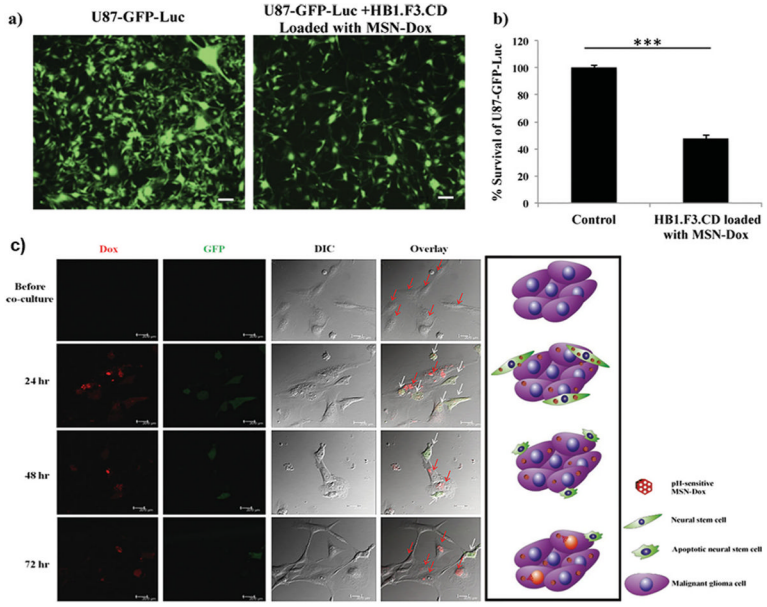

Figure 3.

MSN-Dox-loaded HB1.F3.CD cells conferred toxicity towards U87-GFP-Luc cells. a). Fluorescence images from co-culture of MSN-Dox-loaded HB1.F3.CD cells and U87-GFP-Luc cells. GFP signal corresponds to viable U87-GFP-Luc cells only. Scale bar: 200 μm. b). Luciferase activity assay results at 96 h (***$p<0.001$). c). Confocal images of GFP-labeled MSN-Dox-loaded HB1.F3.CD cells co-cultured with U87 cells. (Red arrows = U87 glioma cells; White arrows = HB1.F3.CD cells.)

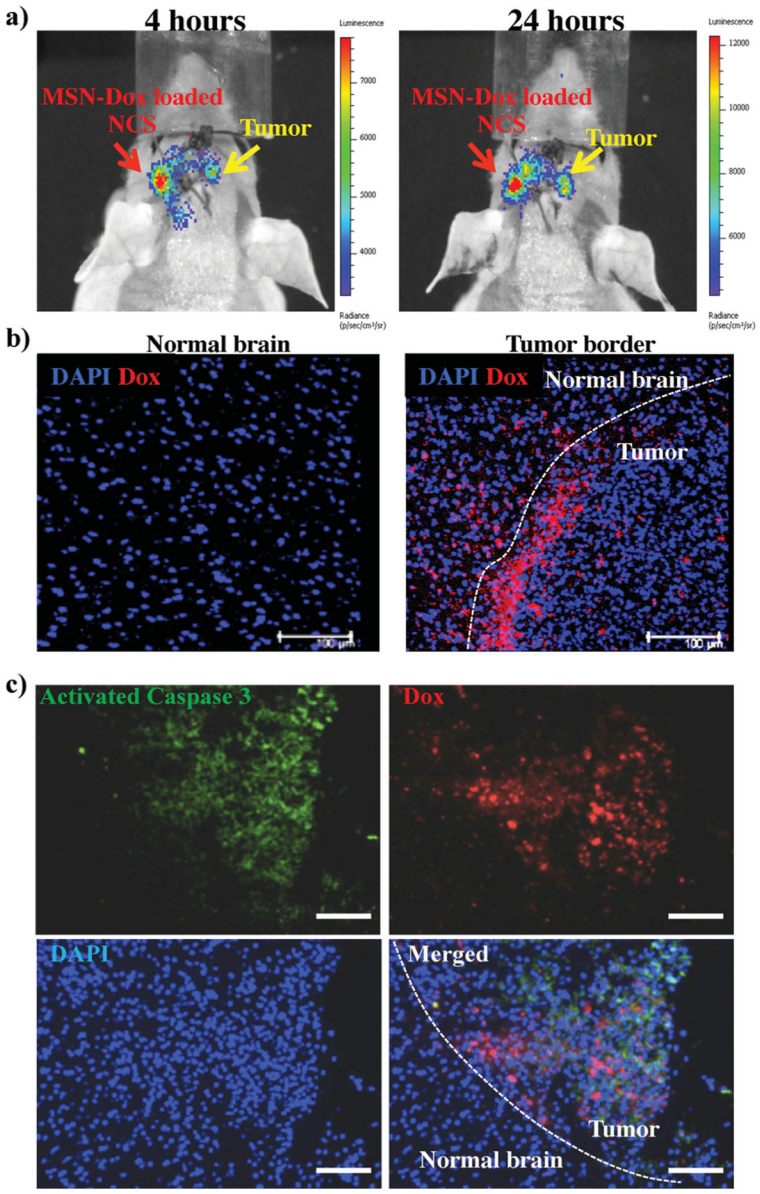

Figure 4.

In vivo tumor-tropic migration of luciferase-labeled HB1.F3.CD cells loaded with MSN-Dox. a) Bioluminescent images of a mouse implanted with a xenograft U87 brain tumor after contralateral injection of MSN-Dox-loaded HB1.F3.CD cells expressing luciferase. b) Confocal images of brain sections taken 3 days after contralateral injection of MSN-Dox-loaded HB1.F3.CD cells. (Dox = red; Nuclei = DAPI). c) Apoptosis within the tumor was assessed via caspase-3 immunofluorescence staining (Activated caspase-3 = green; Dox = red). Scale bar: 100 μm.

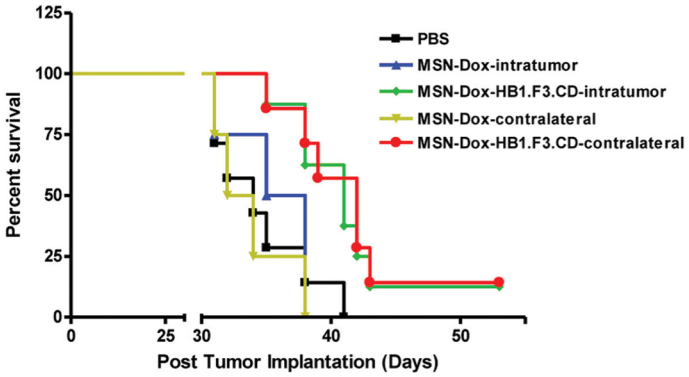

Therapy	Median Survival	p^1	p^2	p^3	p^4
PBS	34 days	Referent			
MSN-Dox-intratumor	36.5 days	0.76	Referent		
MSN-Dox-HB1.F3.CD-intratumor	41 days	**0.009**	**0.03**	Referent	
MSN-Dox-contralateral	33 days	0.66	0.42	**0.005**	Referent
MSN-Dox-HB1.F3.CD-contralateral	42 days	**0.007**	**0.02**	0.79	**0.005**

Figure 5.

Prolonged survival of mice after MSN-Dox loaded HB1.F3.CD cell administration in a xenograft U87 glioma model via intratumoral and contralateral injections. Phosphate buffered saline (PBS) and MSN-Dox treated groups were included as the controls.

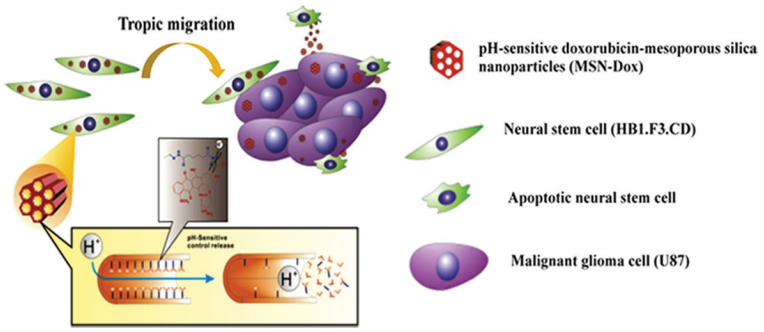

Scheme 1.
Schematic of the pH-senstive MSN-Dox-loaded neural stem cell delivery system.